Honda Research Institute EU
Honda Research Institute Europe GmbH
https://www.honda-ri.de/

Enhancement of interfacial instabilities by solid particles during fast stretching of a liquid suspension bridge

Philipp Brockmann, Hatim Ennayar, Max Lannert, Xulan Dong, Yuhao Cao, Sebastian Brulin, Ilia Roisman, Jeanette Hussong

2024

Preprint:

This is an accepted article published in 16th International Conference on Liquid Atomization and Spray Systems 2024. The final authenticated version is available online at: https://doi.org/[DOI not available]

Interfacial instabilities in a fast stretched suspension bridge with and without particle pre-structuring

Philipp Brockmann*[1], Hatim Ennayar[1], Max Lannert[1], Xulan Dong[1], Yuhao Cao[1], Sebastian Brulin[2], Ilia V. Roisman[1] and Jeanette Hussong[1]

[1]Institute for Fluid Mechanics and Aerodynamics, TU Darmstadt, Darmstadt, Germany
[2]Honda Research Institute Europe, Offenbach, Germany

Keywords
Liquid bridge, interfacial instabilities, suspension

Abstract
In this experimental study, the rapid stretching dynamics and interfacial instabilities of a suspension liquid bridge are studied using a high-speed video system. The bridge is formed between two parallel plates with an initial gap width ranging from 30 to 60 µm. One of the plates is fixed while the second plate moves with a constant acceleration whose magnitude reaches 180 m/s^2. The particle size in the suspensions is varied from 6 to 40 µm. Fast stretching of a viscous liquid bridge may lead to the emergence of the interfacial instability of the bridge meniscus, resulting in the formation of fingers. In this study, it is demonstrated that the the presence of particles amplifies the number of fingers during the initial stretching phase. Furthermore, particles contribute to the emergence of additional secondary fingers in the later stages of the stretching process, strongly increasing the overall finger number. These findings highlight a fascinating phenomenon: the presence of particles triggers the formation of secondary liquid bridges around the primary one. We establish a correlation between the number of bridges and both the particle volume fraction and size. Remarkably, intermediate particle sizes (15 µm) lead to the highest number of secondary bridges, while the smallest particles (6 µm) generate only a few. Furthermore, this study reveals that particles can organize into periodic agglomerations or structures when the liquid is compressed during the experiment preparation. The presence of these structures results in the even distribution of secondary bridges and predefines the spatial locations of the fingers.

Introduction

Liquid bridge stretching refers to the elongation of a thin column of liquid connecting two solid surfaces whose distance increases [1,2]. This phenomenon is relevant to numerous applications in different fields, including characterization of rheological properties of materials [3], flow manipulation in microfluidics [4,5,6], in biomedical [7,8] and chemical engineering, physics [9],[10] and aerospace engineering [11,12,13,14].

The flow in the stretching bridge is governed by the inertial effects, viscous stresses, surface tension and influenced also by the effects associated with the wetting properties of the substrates. The stretching behavior of a liquid bridge has been studied both experimentally and theoretically, with several models proposed to describe the behavior [1,15,16].

During the stretching, the meniscus of the liquid bridge may become unstable and break up into multiple thinner strands, resulting in a finger-like pattern. This behavior is mainly caused by the pressure gradient at the meniscus interface and is known as fingering instability [17]. The behavior of liquid bridges can be significantly affected by the presence of a few suspended particles in the liquid. Even at low solid volume fractions, of about 1-3 %, where the volume fraction does not affect the viscosity, particles can induce disturbances that lead to an accelerated thinning and breakup of the bridge [18]. In general, when a liquid bridge containing particles is stretched, particles can form local agglomerations which lead to the formation of

sharp local constrictions, void of particles, which rapidly break down and lead to an accelerated breakup compared to a pure liquid [19,20]. These local constrictions are also referred to as necks [21]. Larger particles were found to result in an earlier breakup than smaller particles [22]. Moreover, for high shear rates and high volume fractions, particles may block each other and jamming might occur in the liquid bridge leading to its abrupt breakup [19]. While many works so far focused on the behavior of monodisperse suspensions with Newtonian carrier fluids, recently also polydisperse suspensions as well as non-newtonian fluids become the subject of research [23,24,25].

The fingering instability observed during the liquid bridge stretching (radial inward flow in a Hele-Shaw cell), is often considered a Saffman-Taylor instability. This type of instability occurs when a less viscous fluid is injected into a more viscous fluid. In the reversed case, the injection of a more viscous liquid in a less viscous liquid (radial outward flow in a Hele-Shaw cell) is stable. However, in the latter (stable) case, the presence of particles can induce instabilities [26,27,28]. The mechanism responsible for particle-induced fingering is attributed to the accumulation of particles at the fluid-fluid interface (meniscus), resulting in a gradient of effective viscosity which induces miscible fingering [26,27]. Shear-induced migration is the key physical mechanism behind the particle accumulation causing the instabilities [27].

In this paper, we investigate how particles affect the dynamics of liquid bridge stretching, particularly for very small initial gap heights and high accelerations. This study focuses on the effects of particles on fingering instability and filament formation. The initial bridge heights are varied in the experiments starting from is $H_0 = 45$ μm and stretching accelerations reached to $a = 160$ m/s^2. The number of fingers and the number of filaments are measured at various operational conditions, suspension concentrations and particle size.

Experimental setup and data processing

All experiments performed within this study are based on a rapidly stretched liquid bridge forming between two horizontally aligned substrates [29]. A sketch of the experimental setup is shown in Fig. 1. The main component of the stretching apparatus is the linear drive, providing accelerations up to 180 m/s^2 reliably [30,31]. Two separate high-speed video systems are utilized for observation. The first high-speed camera Photron T1340, labeled (1) in Fig. 1, with a pixel size of 13.5 μm records the liquid bridge from the top through the transparent upper substrate (2). A frame-rate of 4000 fps and a resolution of 1024 px $\times$ 976 px, operated in pixel binning mode, is chosen for the experiments and a field of view of 27.95 mm $\times$ 26.6 mm with a spatial resolution of 27.3 μm/px is achieved. A coaxial illumination (3) is realized with a green High Power LED, ILA iLA.LPS v3, with a wavelength of $\lambda \approx 532$ nm. A dichroic mirror plus two band-pass filters, mounted on a filter cube (4), Thorlabs DFM1/M, permit directing the light through the objective (5), Infinity Photo-Optical IF-3, $M = 1\times$, as well as filtering the fluorescence signal [32,33]. The images generated with a high-speed camera (1) are referred to as the top view. The second high-speed camera (6), Phantom Miro Lab 110 with a pixel size of 20 μm records the side profile using a telecentric objective (7) and a telecentric white light LED (8). The images generated with this camera are hereafter referred to as side view. The camera is operated with a frame-rate of 4000 fps and a resolution of 768 px $\times$ 480 px such that a field of view of 20.2 mm $\times$ 16.62 mm with a spatial resolution of 26.31 μm/px is obtained.

The droplet is applied on the lower substrate by scooping it with a custom-designed spoon. After applying the droplet the substrates are brought close to each other, resulting in a squeezing process of the droplet. The distance between the substrates is then measured with a confocal sensor, Micro Epsilon IFS2407-0.1 (9) with an accuracy of up to 3 nm. Hence, the stretching experiment is performed by accelerating the lower substrate (10).

For obtaining a density and refractive index matched (RIM) suspension with PMMA particles of 6, 15, 30, and 40 μm diameter (Microbeads), the recipe proposed by [34] and utilized by

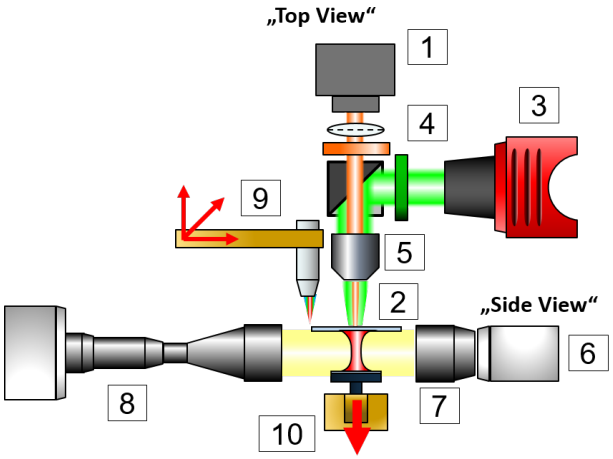


Figure 1: Schematic configuration of the liquid bridge stretching experiment: 1) High speed camera, 2) Transparent upper substrate, 3) LED, 4) Filter cube with filter set and dichroic mirror, 5) Microscope objective, 6) High speed camera, 7) Telecentric obective, 8) Telecentric illumination, 9) Confocal sensor on x,y,z traverse, 10) Linear actuator

[33] was employed. This refractive index matched liquid is a ternary mixture of 26.46 wt% water, 32.30 wt% glycerin and 41.24 wt% ammonium thiocyanate and has a refractive index of $n_{\mathrm{RIM}} = 1.4882$, a density of $\rho_{\mathrm{RIM}} = 1190$ kg/m^3 and a dynamic viscosity of $\eta_{\mathrm{RIM}} = 4.99$ cP. The surface tension was measured with a DataPhysics DCAT tensiometer as $\sigma = 49$ mN/m[1]. The (bulk) solid volume fraction or particle volume fraction is defined as $\Phi = V_{\mathrm{particles}}/V_{\mathrm{total}}$. Here $V_{\mathrm{particles}}$ is the volume of the particles and V_{total} is the combined volume of liquid and particles ($V_{\mathrm{total}} = V_{\mathrm{particles}} + V_{\mathrm{liquid}}$). For rendering the particles visible for the camera, 25 % to 50 % of them have been dyed with Rhodamin B.

The MATLAB Image Processing Toolbox is utilized to determine the number of fingers in top-view grayscale images by use of binarization and skeleton detection routines [35]. All detected fingers are checked manually and corrected if necessary. Like in [17], we consider the number of fingers that form at the beginning of the stretching process, when the fingers just appear. Here, the observed bridge radius is at about 90 % of the initial radius. An exemplary result of the counted number of fingers N_f is depicted in Fig. 2b at 0.0055s.

The filaments are identified by the formation of circular blobs, as can be seen in Fig. 2b at 0.015 s. The number of filaments is counted manually.

Observations of the Phenomena

The presence of particles can have a significant impact on the fingering at the meniscus interface and can lead to a significant increase in finger number at low capillary numbers, depending on the particle size. Moreover, in a suspension regularly or irregularly distributed multiple bridges or filaments can occur. They usually appear at the outer rim of the droplet as well as along the fingers. Thereby, it is observed that the most outward filaments break up at first, followed by the intermediate filaments and the central filament breaks up last, which can be seen from the time series depicted in Fig. 2a. From the top view, the secondary filaments appear as round dots at the outer edge of the droplet as depicted exemplary in Fig. 2b at t = 0.015s. The cavities present in the central region at 0.0055s represent the onset of cavitation.

Furthermore, the presence of particles also can induce instabilities during the compression of the droplet during the experiment preparation, prior to the stretching experiment. This results in an azimuthal fluctuation of particle concentration. This is shown exemplarily in Fig. 3. As can

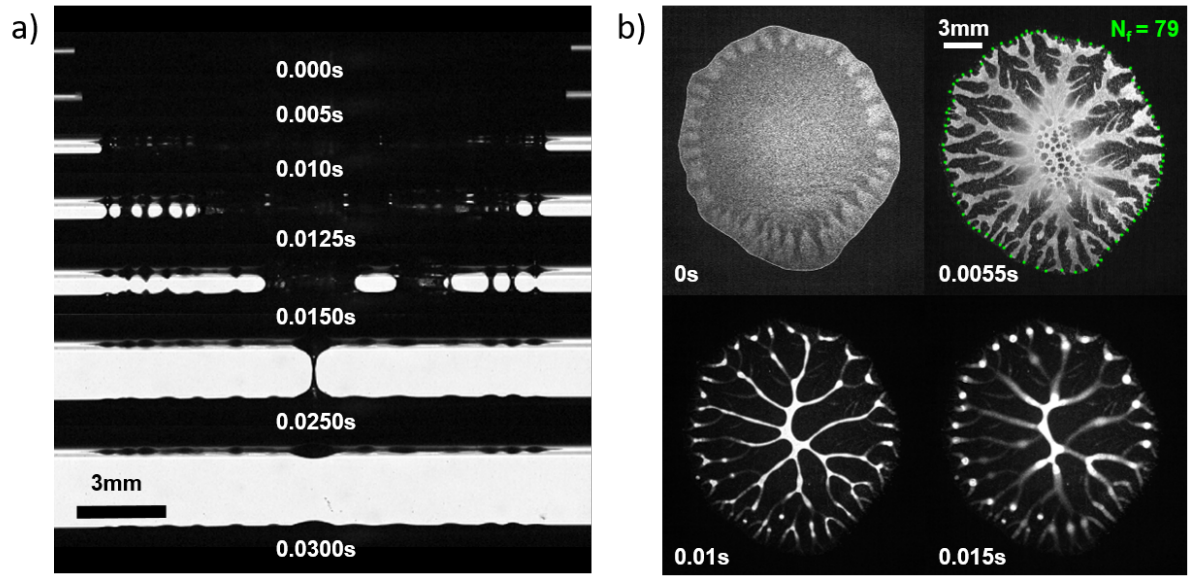


Figure 2: a) Temporal evolution of the stretching experiment. Time stamps are given on the lower plate. The fluid is a 33 % suspension with 15 μm particles at 5 m/s^2. b) Selected images from the top view corresponding to a). The number of fingers N_f, is indicated at 0.0055s with green dots.

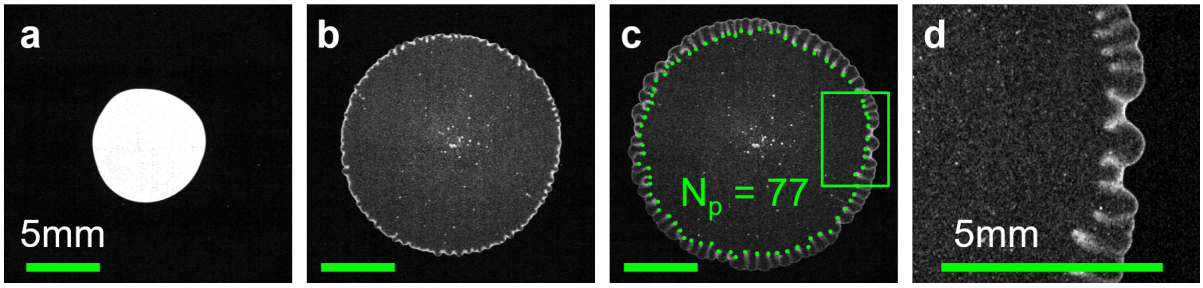


Figure 3: Development of interfacial instability during the drop-squeezing before the experiment (bright regions correspond to a higher concentration of particles). d shows a close-up of c. The number of concentration peaks N_p is given in c, with individual peaks highlighted by green dots.

be seen, as the droplet expands radially and the gap height decreases, instabilities develop at the interface ultimately resulting in a wavelike pattern of particle concentration similar to that described by [27]. This pattern is referred to as ``pre-structure'' in the following. The number of detected concentration peaks is hereafter referred to as N_p as indicated in Fig. 3c.

Results

When dealing with pure liquids, a single bridge typically forms during the stretching process, gradually contracting until the interface becomes unstable and a fingering pattern emerges. The likelihood of this pattern depends on factors such as the capillary number and dimensionless gap height [16],[17]. According to [17] the maximum finger number can be estimated based on the capillary number defined as:

$$Ca = \frac{\sqrt{a}\mu R_0}{\sqrt{2H_0}\sigma}, \tag{1}$$

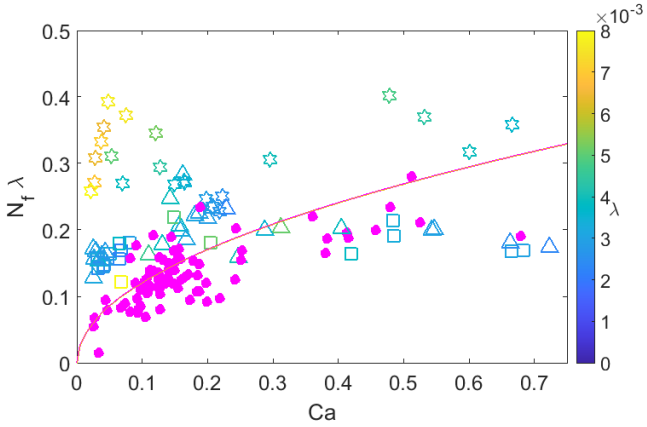


Figure 4: Non-dimensional number of fingers $N_f\lambda$ as a function of the capillary number Ca for suspensions of the concentration $\Phi = 28$ %. Squares correspond to $d_p = 6$ μm, triangles: $d_p = 15$ μm, and hexagons: $d_p = 30$ μm. Colormap indicates λ values. Magenta dots = pure liquid (glycerol water and RIM). $32\,\mu\text{m} \leq H_0 \leq 63\,\mu\text{m}$ and $0.025\,\text{m/s}^2 \leq a \leq 80\,\text{m/s}^2$.

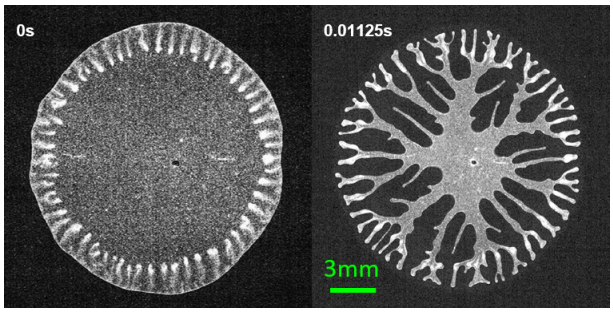


Figure 5: "Lock-in" effect. The location of fingers at $t = 0.01125$ s is essentially identical to the location of concentration peaks of the pre-structure ($t = 0$) for smaller and intermediate particle sizes ($\Phi = 28$ %, $a = 0.5$ m/s^2, $d_p = 6$ μm).

where a, R_0, H_0 denote the acceleration, the initial radius of the bridge, and the initial gap height, respectively. With this capillary number the maximum (normalized) finger $N_f\lambda$ number can be estimated [17] as:

$$N_f\lambda \approx 0.38\sqrt{Ca} \tag{2}$$

where $\lambda = H_0/2R_0$. This estimation is valid for capillary numbers much smaller than unity.

In Fig. 4, we show $N_f\lambda$ as function of the capillary number Ca. Various values of λ are indicated with colors. All data is for the case with pre-structure. Fig. 4 reveals a very good agreement between equation (2) and the data for pure liquid (RIM and Glycerol-water mixture). Instead, the data for 30 μm particles (hexagon symbols) deviates significantly from equation (2) and reveals significantly higher values of $N_f\lambda$. For 6 μm (squares) and 15 μm (triangles), the finger number $N_f\lambda$ is significantly lower than for large particles and appears to be almost constant, which is due to the ``lock-in" effect. For $Ca < 0.05$ 6 $\mu$m and 15 $\mu$m particles seem to result in the same wavelength due to the ``lock-in" effect. For $0.1 < Ca < 0.25$ a slight increase in $N_f\lambda$ becomes apparent for 15 μm particles.

The ``lock-in" effect can be understood easily by comparing the number of concentration peaks of the pre-structure N_p to the maximum number N_f of detected fingers. We performed such a comparison for 6, 15 and 30 μm particles and obtained an average percentage deviation ($\Delta N = (N_f - N_p)/N_p \cdot 100$) of $\overline{\Delta N} = 0.2\,\% \pm 11\,\%$, $\overline{\Delta N} = 34\,\% \pm 18\,\%$ and $\overline{\Delta N} = 316\,\% \pm 75\,\%$, respectively. The volume fraction was 0.28 % and $\lambda = O(10^-3)$. From these values of $\overline{\Delta N}$

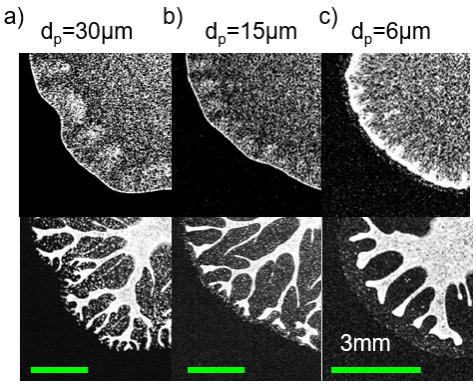


Figure 6: Finger shapes for different particle sizes at $a = 20$ m/s^2 and $\Phi = 28.5$ % volume fraction.

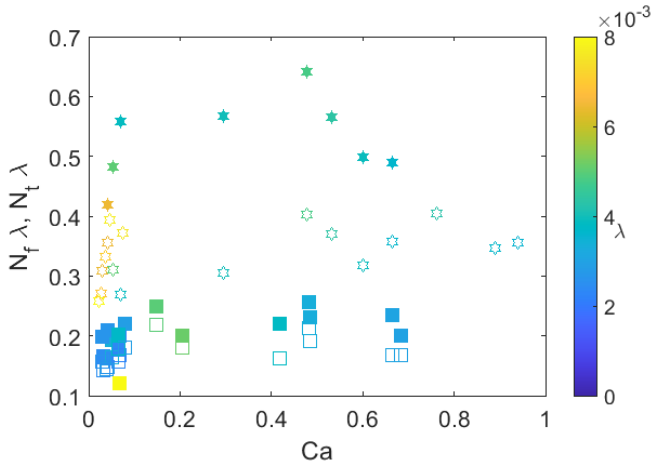


Figure 7: Total number of fingers N_t and the maximum number of outer fingers N_f as a function of the capillary number Ca. Hexagon symbols indicate $d_p = 30\,\mu$m, squares indicate $d_p = 6\,\mu$m. Filled symbols correspond to N_t, hollow symbols: N_f. The suspension concentration $\Phi = 28.5$ % is the same for all the experiments. The values of λ are given in the colorbar. The gap height H_0 was kept between $39\,\mu\text{m} \leq H_0 \leq 63\,\mu$m, with the acceleration between $0.025\,\text{m/s}^2 \leq a \leq 80\,\text{m/s}^2$.

it is clear, that the wavelength of the fingers, is almost identical to the wavelength of the concentrations peaks for 6 μm particles as can also be seen from Fig. 5. This is a strong indicator that the wavelength of the fingers is determined by a type of ``channeling'' happening in between the concentration peaks for 6 μm particles. In fact, velocity measurements by means of PIV confirmed, that the velocity of particles is significantly slowed down at the locations where the concentration peaks are located.

In general we assume that larger particles tend to cause larger disturbances such that they can overwrite the wavelength that is predefined by the pre-structuring. This can be seen in Fig. 6 where we show fingertips for different particle sizes. As can be seen for 6 μm particles, the fingers are well rounded, while for 15 μm the fingers are more blunt and hammer-shaped. Finally, for 30 μm particles, it can be seen that much smaller fingers are superimposed to the concentration peaks of the pre-structure, resulting in an overall larger finger number.

This tendency of larger particles to break the interface tends also to enhance the occurrence of secondary fingers that occur in the inner region of the droplet. These secondary fingers can be seen exemplarily for 6 μm particles in Fig. 5 ($t = 0.01125$ s). In Fig. 7 we compare

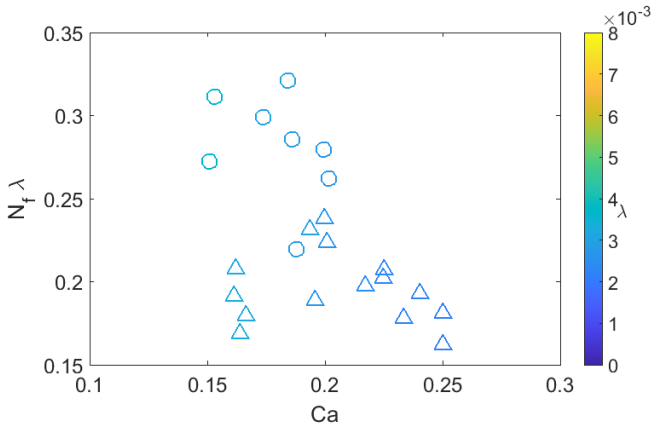


Figure 8: Normalized finger number $N_f\lambda$ with pre-structure (triangles) and without pre-structure (circles) in a 33 % suspension of 15 μm particles. Colormap indicates λ values. The gap height H_0 was kept between $44\,\mu\text{m} \leq H_0 \leq 57\,\mu\text{m}$, with the acceleration being $a = 5\,\text{m/s}^2$.

the number of the secondary fingers and outer fingers. It can be clearly seen, that for larger particles (hexagons) there are much more secondary fingers than for smaller particles (squares).

In Fig. 8 we show the normalized maximum finger number measured with and without particle pre-structure for a 33.3 % suspension with 15 μm particles. The particle pre-structure has been removed by rotating the lower plate for 360 degrees. As can be seen, in Fig. 8 without pre-structure $N_f\lambda$ is significantly higher (0.281 ± 0.032) than with pre-structure (0.197 ± 0.022). Hence, if the pre-structure is absent smaller wavelengths can develop.

As mentioned above, at sufficiently high Ca number in a suspension flow the liquid bridge can split into multiple secondary bridges (see the exemplary side views in Fig. 2a). In Fig. 9 we show the number of filaments for different particle sizes and volume fractions as a function of the capillary number. The capillary number has been varied by changes of λ as well as the acceleration. As can be seen, at a capillary number of about 0.1 the number of filaments increases sharply. Thereby, the number of filaments tends to increase with increasing volume fraction for 15 μm particles in between $Ca = 0.1$ and 0.2. However, the data strongly scatters for $\Phi = 0.28$ % which indicates that there is another non-dimensional number important besides Ca. Also, the particle size plays a role in the number of filaments. Our results show that intermediate particles tend to produce the highest number of filaments, while smaller particles tend to produce only a small number of filaments.

It should be further noted that in almost every experiment where secondary filaments were observed, cavitation has also been detected. Hence, there may be a connection between the occurrence of secondary filaments and cavitation, as concluded by Brulin [31] for pure liquid. However, the presence of cavitation does not always yield a significant number of filaments. In pure liquids, the number of filaments tends to be significantly lower than in suspensions, even when pronounced cavitation is present at $Ca > 0.4$ (magenta dots in Fig. 9). Therefore, we conclude that filament formation is mainly caused by jamming of particles associated with high particle volume fractions, leading to blockage of the flow in the radial direction and ultimately causing flow separation. The likelihood of jamming or clogging, and hence filament formation, depends on the ratio of particle size to gap height. According to the literature, particles that are either very small or very large compared to the channel are less likely to jam than intermediate-sized particles ($d/D = 0.3 \ldots 0.4$), as the latter most efficiently lead to arch formation [35,36]. Consequently, for the smallest particle size ($d/H_0 \approx 0.13$), the likelihood of clogging is much less, and therefore filament formation is much lower, even in the presence of pronounced pre-

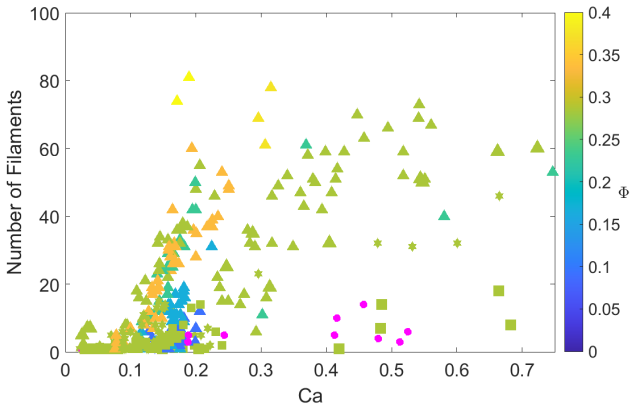


Figure 9: Number of filaments as a function of the capillary number. Squares, Triangles, and Hexagons represent 6, 15, and 30 μm particles, respectively. Colormap indicates λ values. Magenta dots represent results for pure liquid (glycerol water and RIM). The gap height H_0 was kept between $29\,\mu\text{m} \leq H_0 \leq 65\,\mu\text{m}$, with the acceleration between $0.025\,\text{m/s}^2 \leq a \leq 80\,\text{m/s}^2$.

structuring. To underline this conclusion, in cases of pre-structuring, we always observed that secondary filaments form at the location of the highest particle concentration, where jamming is most probable. Regarding the number of filaments, it was found that pre-structuring leads to a slightly higher number of filaments. However, this needs to be investigated further.

Summary and conclusion

In the present work the effect of particles on the filament formation and the fingering instability during the fast stretching on a liquid bridge was investigated.

- We showed that before the stretching, the suspension can exhibit an inhomogeneous distribution of particles, which arises due to an instability that occurs when the substrates are pressed together to prepare the experiment. The resulting distribution of particles is periodic in azimuthal direction and is referred to as pre-structure.
- We have discovered that this pre-structure predefines the number of fingers for small particles ($d_p = 6\ \mu$m). For small particles, even for an increasing capillary number, the number of fingers remains identical to the number of peaks in the pre-structure. At higher capillary numbers, this results in a lower number of fingers compared to the pure liquid. Instead, the large disturbances created by relatively larger particles ($d_p = 15\ \mu$m) appear to overwrite the wavelength imposed by the pre-structure and result in a significantly larger number of fingers compared to smaller particles, as well as to the pure liquid.
- The number of filaments increases with increasing capillary number. Moreover, the intermediate particles, result in a significantly larger number of filaments compared to small or large particles.

Acknowledgement

This project is funded by the Deutsche Forschungsgemeinschaft (DFG, German Research Foundation) - Project Number 265191195 - SFB 1194, sub- project A03. Hatim Ennayar is funded by the Deutsche Forschungsgemeinschaft (DFG, German Research Foundation) - project number 237267381 - TRR 150, sub-project A07.

variable	definition
a	acceleration (m/s^2)
Ca	capillary number (-)
d_p	particle diameter (m)
H_0	initial gap height (m)
N_f	(max.) number of fingers (-)
N_p	number of peaks in pre-structure (-)
R_0	initial bridge radius (m)
t	time (s)
$\lambda = H_0/2R_0$	initial aspect ratio (-)
μ	dynamic viscosity (cP)
σ	surface tension (N/m)
Φ	particle volume fraction (-)

Nomenclature

References

[1] Zhang, X. , Padgett, R. S., and Basaran, O. A., ``Nonlinear deformation and breakup of stretching liquid bridges,'' *Journal of Fluid Mechanics*, vol. 329, pp. 207--245, 1996.

[2] Roisman, I. V., Abboud, M., Brockmann, P., Berner, F., Berger, R., Rothmann-Brumm, P., Sauer, H. M., Dörsam, E., and Hussong, J., ``Forced flows in liquid bridges,'' *Current Opinion in Colloid & Interface Science*, p. 101738, 2023.

[3] McKinley, G. H. and Sridhar, T., ``Filament-stretching rheometry of complex fluids,'' *Annual Review of Fluid Mechanics*, vol. 34, no. 1, pp. 375--415, 2002.

[4] Marston, P. L. and Thiessen, D. B., ``Manipulation of fluid objects with acoustic radiation pressure,'' *Annals of the New York Academy of Sciences*, vol. 1027, no. 1, pp. 414--434, 2004.

[5] Feng, J., Song, Q., Zhang, B., Wu, Y., Wang, T., and Jiang, L., ``Large-scale, long-range-ordered patterning of nanocrystals via capillary-bridge manipulation,'' *Advanced Materials*, vol. 29, no. 46, p. 1703143, 2017.

[6] Wu, L., Dong, Z., Li, F., and Song, Y., ``Designing laplace pressure pattern for microdroplet manipulation,'' *Langmuir*, vol. 34, no. 2, pp. 639--645, 2018.

[7] Wang, L., Qiu, M., Yang, Q., Li, Y., Huang, G., Lin, M., Lu, T. J., and Xu, F., ``Fabrication of microscale hydrogels with tailored microstructures based on liquid bridge phenomenon,'' *ACS Applied Materials & Interfaces*, vol. 7, no. 21, pp. 11134--11140, 2015.

[8] Ehrig, S., Schamberger, B., Bidan, C. M., West, A., Jacobi, C., Lam, K., Kollmannsberger, P., Petersen, A., Tomancak, P., Kommareddy, K., *et al.*, ``Surface tension determines tissue shape and growth kinetics,'' *Science advances*, vol. 5, no. 9, p. eaav9394, 2019.

[9] Sakata, T., Terasaki, S., Saito, H., Fujimoto, S., Ueno, I., Yano, T., Nishino, K., Kamotani, Y., and Matsumoto, S., ``Coherent structures of m= 1 by low-stokes-number particles suspended in a half-zone liquid bridge of high aspect ratio: Microgravity and terrestrial experiments,'' *Physical Review Fluids*, vol. 7, no. 1, p. 014005, 2022.

[10] Šeta, B., Dubert, D., Massons, J., Gavalda, J., Bou-Ali, M. M., and Ruiz, X., ``Effect of marangoni induced instabilities on a melting bridge under microgravity conditions,'' *International Journal of Heat and Mass Transfer*, vol. 179, p. 121665, 2021.

[11] Weislogel, M. M., Graf, J., Wollman, A. P., Turner, C., Cardin, K., Torres, L., Goodman, J., and Buchli, J., ``How advances in low-g plumbing enable space exploration,'' *npj Microgravity*, vol. 8, no. 1, p. 16, 2022.

[12] Li, J.-C., Lin, H., Li, K., Zhao, J.-F., and Hu, W.-R., ``Liquid sloshing in partially filled capsule storage tank undergoing gravity reduction to low/micro-gravity condition,'' *Microgravity Science and Technology*, vol. 32, pp. 587--596, 2020.

[13] Chen, S., Duan, L., and Kang, Q., ``Study on propellant management device in plate surface tension tanks,'' *Acta Mechanica Sinica*, vol. 37, pp. 1498--1508, 2021.

[14] Nijhuis, J., Schmidt, S., Tran, N. N., and Hessel, V., ``Microfluidics and macrofluidics in space: Iss-proven fluidic transport and handling concepts,'' *Frontiers in Space Technologies*, vol. 2, p. 16, 2022.

[15] Kumar, S., ``Liquid transfer in printing processes: liquid bridges with moving contact lines,'' *Annual Review of Fluid Mechanics*, vol. 47, pp. 67--94, 2015.

[16] Brulin, S., Tropea, C., and Roisman, I. V., ``Pinch-off of a viscous liquid bridge stretched with high reynolds numbers,'' *Colloids and Surfaces A: Physicochemical and Engineering Aspects*, vol. 587, p. 124271, 2020.

[17] Brulin, S., Roisman, I. V., and Tropea, C., ``Fingering instability of a viscous liquid bridge stretched by an accelerating substrate,'' *Journal of Fluid Mechanics*, vol. 899, p. A1, 2020.

[18] Lindner, A., Fiscina, J. E., and Wagner, C., ``Single particles accelerate final stages of capillary break-up,'' *Europhysics Letters*, vol. 110, no. 6, p. 64002, 2015.

[19] Smith, M., Besseling, R., Cates, M., and Bertola, V., ``Dilatancy in the flow and fracture of stretched colloidal suspensions,'' *Nature communications*, vol. 1, no. 1, p. 114, 2010.

[20] Mathues, W., McIlroy, C., Harlen, O. G., and Clasen, C., ``Capillary breakup of suspensions near pinch-off,'' *Physics of Fluids*, vol. 27, no. 9, p. 093301, 2015.

[21] Alexandrou, A. N., Bazilevskii, A., Entov, V., Rozhkov, A., and Sharaf, A., ``Breakup of a capillary bridge of suspensions,'' *Fluid Dynamics*, vol. 45, no. 6, pp. 952--964, 2010.

[22] Château, J., Guazzelli, É., and Lhuissier, H., ``Pinch-off of a viscous suspension thread,'' *Journal of Fluid Mechanics*, vol. 852, pp. 178--198, 2018.

[23] Thiévenaz, V. and Sauret, A., ``Pinch-off of viscoelastic particulate suspensions,'' *Physical Review Fluids*, vol. 6, no. 6, p. L062301, 2021.

[24] Thiévenaz, V., Rajesh, S., and Sauret, A., ``Droplet detachment and pinch-off of bidisperse particulate suspensions,'' *Soft matter*, vol. 17, no. 25, pp. 6202--6211, 2021.

[25] Faletra, M., Marshall, J. S., Yang, M., and Li, S., ``Particle segregation in falling polydisperse suspension droplets,'' *Journal of Fluid Mechanics*, vol. 769, pp. 79--102, 2015.

[26] Tang, H., Grivas, W., Homentcovschi, D., Geer, J., and Singler, T., ``Stability considerations associated with the meniscoid particle band at advancing interfaces in hele-shaw suspension flows,'' *Physical Review Letters*, vol. 85, no. 10, p. 2112, 2000.

[27] Xu, F., Kim, J., and Lee, S., ``Particle-induced viscous fingering,'' *Journal of Non-Newtonian Fluid Mechanics*, vol. 238, pp. 92--99, 2016.

[28] Chen, Y., Luo, R., Wang, L., and Lee, S., ``Self-similarity in particle accumulation on the advancing meniscus,'' *Journal of Fluid Mechanics*, vol. 925, p. A10, 2021.

[29] Asghar, M. H., Brockmann, P., Dong, X., Niethammer, M., Maric, T., Roisman, I., and Bothe, D., ``Asymmetry during fast stretching of a liquid bridge,'' *Chemical Engineering & Technology*, vol. 46, no. 9, pp. 1800--1807, 2023.

[30] Weickgenannt, C., Roisman, I. V., and Tropea, C., ``Pinch-off of a stretching viscous filament and drop transport,'' *New Journal of Physics*, vol. 17, no. 8, p. 083059, 2015.

[31] Brulin, S., *Hydrodynamic investigations of rapidly stretched liquid bridges*. PhD thesis, Dissertation, Darmstadt, Technische Universität Darmstadt, 2020, 2021.

[32] Ennayar, H., Brockmann, P., and Hussong, J., ``Lif-based quantification of the species transport during droplet impact onto thin liquid films: Species transport during droplet impact onto thin liquid films,'' *Experiments in Fluids*, vol. 64, no. 9, p. 148, 2023.

[33] Brockmann, P., Symanczyk, C., Ennayar, H., and Hussong, J., ``Utilizing aptv to investigate the dynamics of polydisperse suspension flows beyond the dilute regime: Applying aptv to polydisperse suspensions flows,'' *Experiments in Fluids*, vol. 63, no. 8, p. 129, 2022.

[34] Bailey, B. and Yoda, M., ``An aqueous low-viscosity density-and refractive index-matched suspension system,'' *Experiments in fluids*, vol. 35, pp. 1--3, 2003.

[35] Fong, A., ``Skeleton endpoints (https://www.mathworks.com/matlabcentral/fileexchange/4251-skeleton-endpoints),'' *MATLAB Central File Exchange*, p. Retrieved June 7, 2023.

[36] Bailey, B. and Yoda, M., ``An aqueous low-viscosity density-and refractive index-matched suspension system,'' *Experiments in fluids*, vol. 35, pp. 1--3, 2003.

[36] López, D., Hernández-Delfin, D., Hidalgo, R. C., Maza, D., and Zuriguel, I. . Clogging-jamming connection in narrow vertical pipes. *Physical Review E*, vol. 102(1), pp. 010902, 2020

[37] Sharp, K. V., and Adrian, R. J. On flow-blocking particle structures in microtubes, *Microfluidics and Nanofluidics*, vol. 1(4), pp. 376-380, 2005